Modeling hot-electron generation induced by electron promotion in atomic collision cascades in metals

Andreas Duvenbeck,[1] Boris Weidtmann,[1] Oliver Weingart,[2] and Andreas Wucher[1]
[1]*Department of Physics, University of Duisburg-Essen, D-47048 Duisburg, Germany*
[2]*Department of Chemistry, University of Duisburg-Essen, D-45117 Essen*
(Received 3 March 2008; revised manuscript received 18 April 2008; published 27 June 2008)

We present a computer simulation model for the investigation of electron promotion processes in atomic collision cascades in metals. The model combines molecular dynamics and molecular orbital calculations to describe the formation of hot electrons in close atomic collisions. We apply this model to a set of collision cascades initiated by the impact of a 5-keV silver atom onto an Ag(111) surface. The calculations show that about 15% of the bombarding energy originally introduced into the solid is dissipated into the generation of hot electrons in close collisions. Furthermore, we find that the nascent excitation energy spectrum closely resembles a power law $f(E_{\mathrm{exc}}) \propto E_{\mathrm{exc}}^{-\delta}$ with exponents $\delta \approx 2-3$.

DOI: 10.1103/PhysRevB.77.245444 PACS number(s): 79.20.Ap, 71.10.Ca, 71.10.Li

I. INTRODUCTION

The bombardment of a solid surface with energetic ions initiates a complex series of atomic collisions among the target atoms. First, the projectile loses energy either by elastic collisions ("nuclear stopping") or via inelastic processes leading to electronic excitations ("electronic stopping"). Moreover, recoiling target atoms will experience the same energy-loss processes, thus producing further recoil atoms, as well as additional electronic excitation. As a consequence, an atomic collision cascade develops in space and time, which may ultimately lead to the release of particles from the surface ("sputtering").[1,2]

In the kiloelectronvolt regime of impact energies investigated here, nuclear stopping is known to be the dominant energy-loss mechanism.[3] Nevertheless, a substantial fraction of the kinetic energy originally imparted to the surface is dissipated via electronic degrees of freedom.[4] Experimentally, this "kinetic excitation" manifests in two different ways. First, electrons are released from the surface either into the vacuum ("kinetic electron emission")[5] or into the solid ("internal electron emission").[6] Second, sputtered particles may leave the surface in electronically excited or ionized states.[7,8] Particularly the formation of secondary ions is important since it forms the basis of secondary ion mass spectrometry[9] as one of the most versatile methods of chemical surface analysis.

A theoretical description of kinetic excitation in atomic-collision cascades requires knowledge of the microscopic particle dynamics within the collision cascade. More specifically, it is important to determine where and when atoms are moving or colliding, as well as the energies involved in these processes. Based on this information, one can assign inelastic energy-loss mechanisms to every moving atom, thus forming a space- and time-dependent source of electronic excitation within the cascade volume. While analytic theories of kinetic electron emission[10] or secondary ion formation[11–20] usually employ relatively coarse statistical averages, the required information can be ideally obtained from molecular dynamics (MD) computer simulations of the cascade dynamics.

In principle, dynamically induced electronic excitation can be described by solving the Schrödinger equation for all nuclei and electrons of the system. Such *ab initio* MD calculations have been successfully performed for small systems containing up to several tens of atoms.[21,22] Unfortunately, the computational effort to describe a system large enough to enclose an ion-impact-induced collision cascade is still clearly beyond what is possible to date. Therefore, it appears promising to combine classical MD simulations with simple models describing kinetic excitation mechanisms. Prominent inelastic energy-loss processes undergone by particles moving in a solid are electronic friction via scattering of quasi-free conduction-band electrons and electron-promotion in close atomic collisions.

To first order, electronic friction can be described by the Lindhard model of electronic stopping,[23] which treats the kinetic excitation in terms of the dielectric response of a free-electron gas to the passage of a moving atom. The resulting energy loss experienced by the atom can be described as an effective friction force that is proportional to the particle velocity.

The electron promotion mechanism is based upon the physical picture that during a close atomic-collision transient quasimolecular orbitals (MO) are formed with eigenenergies that vary as a function of the interatomic distance.[24] In a "diabatic" picture, some of these orbitals may be promoted to higher energies while the atoms approach each other. Whenever an occupied MO increases in energy such that it exceeds the Fermi level, resonant autoionizing transitions to free conduction-band states become possible,[25] thereby generating a hot electron while leaving a vacancy in the MO.

Both electronic friction and electron promotion have been incorporated into MD simulations of atomic collision cascades before.[21,26–40] In many cases,[32,38–40] electronic friction was merely acknowledged as an energy-loss mechanism influencing the nuclear dynamics, while the resulting electronic excitation was largely ignored. Only recently this process has been incorporated into microscopic calculations of the generation and transport of electronic excitation in atomic collision cascades.[4] In the case of electron promotion, practically all published work[26,27,35–37] was strictly focused

on the vacancy-formation process, while the fate of the liberated electron was not considered.

The present study aims at a detailed investigation of the electron promotion mechanism as a source of hot electrons in states above the Fermi level, which operates in addition to the electronic friction mechanism. Using a combination of classical MD simulations and diabatic correlation curves determined from *ab initio* MO computations, we calculate the total amount of electronic excitation energy generated by electron promotion for a set of 120 collision cascades initiated by the individual impact of a 5-keV Ag atom onto an Ag(111) surface. Using simple assumptions regarding the autoionizing transition rates, we then derive the excitation spectrum of the hot electrons generated within the cascade volume.

II. MODEL

The microscopic particle kinetics within the atomic-collision cascade initiated by a 5-keV silver atom impinging onto an Ag(111) crystallite under normal incidence are modeled by means of MD computer simulations described in detail earlier.[41–44] In short, for the projectile and all target atoms, the Newtonian equations of motion are numerically integrated in order to follow the time evolution ("trajectory") of the particle system up to a maximum simulated time of 3 ps after the projectile impact. The interactions among the ensemble of particles are described using the MD/MC-CEM potential[45] for silver. The model crystallite employed in the calculations consists of 4500 atoms arranged in 18 layers. The system size is chosen as such to ensure that for practically all trajectories studied here, the collision cascade remains completely enclosed during the first 150 fs after the projectile impact, which is essential for the formation of hot electrons by electron promotion processes. Moreover, it was shown previously[42] that calculations for selected trajectories using larger crystal sizes produce practically identical results.

In order to incorporate the electronic degree of freedom into the MD simulation, we assume the atomic collision cascade to be embedded into a quasi-free, nondegenerate Fermi gas representing the metal conduction electrons. Electronic friction is treated within the Lindhard model[23] yielding a velocity proportional friction force acting on each particle moving within the solid. The friction force naturally enters the equations of motion. For details on the inclusion of Lindhard friction into the MD, the reader is referred to Refs. 21 and 29.

Electron promotion is treated on the basis of the curve-crossing model of Fano and Lichten.[24] During a close gas-phase collision of two atoms, the overlap of wave functions leads to the formation of quasi-MO, whose energies vary as a function of the interatomic separation r. In a diabatic picture, crossings between different MO levels may occur and allow for electron exchange from one level to another. As originally pointed out by Joyes,[46] this mechanism may also be applied for hard collisions within a *solid*, with the distinct difference that in this case not only level crossings but also crossings between a MO level and a band may occur. Whenever one initially occupied MO increases in energy such that

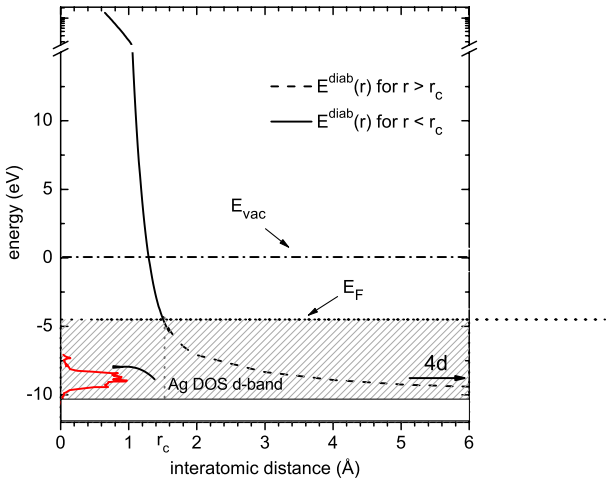

FIG. 1. (Color online) Diabatic MO energy versus interatomic distance of two silver atoms colliding within solid silver (taken from Ref. 4).

is exceeds the Fermi level, the electron may undergo a resonant autoionizing transition from the promoted orbital into a delocalized free conduction-band state. The delocalization of the hot electron is assumed to occur on a subfemtosecond time scale. Therefore, a reverse transition from the conduction-band state into the MO is highly improbable and, hence, neglected. The electronic transition is accompanied by the formation of a vacancy in the MO. On the time scale of a few femtoseconds, this vacancy will stay localized as an inner shell hole at one of the colliding atoms. At later times the hole will be shared among neighbored particles and finally delocalize in the valence band. It should be noted here, that in the course of the collision cascade, these holes may de-excite via Auger transitions, which constitute an additional, indirect source of electronic excitation. This energy is taken into account in our simulations and leads to the limit of the average excitation energy for large values of Δ in Fig. 3.

For a violent binary collision of two isolated Ag atoms in the vacuum, we have calculated[4] that the $9\sigma_u$ MO evolving from the atomic $4d-4d$ level energetically shifts upward with decreasing interatomic distance. The corresponding diabatic energy curve $E^{\mathrm{diab}}(r)$ constructed from these (adiabatic) calculations is depicted in Fig. 1.

In order to apply $E^{\mathrm{diab}}(r)$ for a hard binary collision within a silver solid, the diabatic curve has to be correlated with the band structure of silver. This is done by embedding the potential curve into the energy scheme of silver such that for $r \rightarrow \infty$ $E^{\mathrm{diab}}(r)$ converges to the "center of gravity" of the density of states of the d band. The density of states data is taken from tight-binding calculations carried out by Zhang *et al.*[47] The values for the Fermi energy (E_F=5.4 eV), as well as the work function (Φ=4.74 eV), are adopted from literature.[48]

Figure 1 shows that $E^{\mathrm{diab}}(r)$ energetically crosses the Fermi energy at an interatomic distance r_c=1.5 Å. For $r < r_c$, $E^{\mathrm{diab}}(r)$ can be parametrized (solid line in Fig. 1) as[4]

$$E^{\mathrm{diab}}(r) = a + b/\cosh(\gamma r) \tag{1}$$

with a=−7.1 eV, b=1657 eV, and γ=4.75 Å^{-1}. Let $r^* < r_c$ be the internuclear distance at which the electronic tran-

sition takes place. Then, we define the excitation energy $E_e(r^*)$ of the hot electron generated by autoionization as

$$E_e(r^*) = E^{\text{diab}}(r^*) - E_F. \tag{2}$$

Taking into account the additional energy E_h that is stored in the generated d hole, we arrive at a total excitation energy

$$E_{\text{exc}} = E_e + E_h \tag{3}$$

produced in this collision. The value of E_h is taken as the energy difference between E_F and the energy corresponding to the center of gravity of the density of states in the d band of silver. In view of Eqs. (2) and (3) it becomes directly obvious that for each hard collision, the total amount of generated excitation energy strongly depends on r^*.

In Ref. 4 we have presented a stochastic Landau-Zener approach to derive an analytical expression for the transition probability $p(r)$ as a function of interatomic distance. However, besides the detailed collision dynamics directly accessible from the MD calculation, the numerical evaluation of $p(r)$ requires exact knowledge about the width of the energy gap in an avoided crossing between the promoted MO and a free conduction-band state. At least for the system studied here, this energy gap constitutes an unknown parameter. In order to obtain an upper estimate for the total excitation energy generated by electron promotion in an atomic collision cascade, the calculations in Ref. 4 were carried out under the assumption that electronic transitions always occur with unit probability at the minimum internuclear distance in each collision. In the following, this approximation will be referred to as distance of closest approach (DCA).

Here, we present a more sophisticated approach to treat the transition: The essential physics of the resonant autoionizing transition may be described in terms of a localized MO state interacting with the continuum of delocalized conduction-band states. The overlap of the corresponding wave functions transforms the MO into a virtual bound state (VBS) of finite width Δ, which then determines the transition rate $\Gamma = 2\Delta/\hbar$. In principle, Γ can be derived from Fermi's golden rule as

$$\Gamma(E) = \frac{2\pi}{\hbar}|V_{ik}(E)|^2 \rho(E) \tag{4}$$

with V_{ik} denoting the matrix element for the resonant transition from the MO i of energy E to equienergetic conduction-band states k with a density $\rho(E)$. While the density of states of the three-dimensional electron gas simply obeys a $\sqrt{E}$ dependence, a physically meaningful evaluation of the matrix elements V_{ik} requires the knowledge of the diabatic MO during the close collision. Although it is in principle possible to approximate diabatic MOs using *ab initio* methods,[49] those calculations are extremely complicated and, hence, clearly outside the scope of the present paper. Therefore, as a first approximation we employ a constant-level width Δ, which is taken from experimental data. This procedure is equivalent to the assumption of an energy-independent density of states $\rho(E)$ and a constant matrix element V_{ik} in Eq. (4).

In addition, it should be noted here that we only allow one electronic transition to take place during a hard collision. In principle, a twofold electronic excitation may be physically possible due to the fact that the promoted diabatic orbital is occupied with two electrons. However, the generation of a (first) hot electron is accompanied by the formation of a vacancy in the MO. We assume that this vacancy alters the eigenenergy of the diabatic MO such that it falls below the Fermi energy and, thus, the generation of a second hot electron is prohibited.

For a given level-broadening Δ, the electronic transitions are treated within the MD code using the following Monte Carlo algorithm: At each MD time step, which is chosen small enough to ensure that no particle moves more than 0.01 Å per integration step, the distribution of interatomic distances among all atoms is analyzed. If there is a pair of atoms with an internuclear distance r below r_c, these atoms are flagged to take part in a hard binary collision, which is indexed for quick identification. As long as r remains below r_c, in each of the following time steps i of length dt_i, a random number $a_i \in [0,1]$ is generated and the resonant electronic transition is assumed to occur if $a_i < \Gamma \cdot dt_i$. In that case, the corresponding collision is flagged in order to prohibit a second excitation during one single-close encounter. A detailed analysis of individual hard-collision processes shows that typical transition probabilities within one time step are in the range from approximately 5×10^{-3} to 1.25×10^{-2} and, thus, by two to three orders of magnitude smaller than one. This ensures the applicability of our Monte Carlo approach.

Let j be the index of the time interval where the transition takes place, then the excitation energy is given by $E_{\text{exc}}[r(t_j)]$. In the MD-step $(j+1)$ directly following the transition, this excitation energy is subtracted from the potential energy by artificially increasing the interatomic distance of the colliding atoms such that the resulting potential energy deficit matches the excitation energy. We are aware that this artificial enforcement of energy conservation must be considered as a rough approximation. A more realistic and self-consistent treatment of the energy dissipation would require taking into account the change of the potential energy surface following the excitation. Even for an isolated Ag_2 dimer, this would require a very large quantum chemical effort. Since the excitation energy density is strongly space and time dependent, it would be necessary to recalculate the interaction potential at each point in space and time separately from *ab initio* methods. Such a calculation does not appear possible to date.

III. RESULTS

The calculation of particle dynamics, as well as electronic excitations as described above, has been carried out for the bombardment of an (111)-oriented silver crystallite with a 5-keV monoatomic silver projectile.

In order to account for the statistical nature of the sputtering process, the lateral impact point of the projectile on the surface has been varied. The hexagonal symmetry of the (111) surface allows a confinement of the lateral distribution

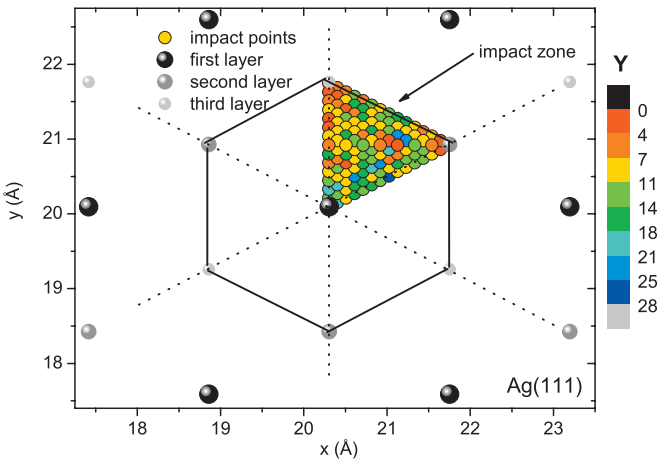

FIG. 2. (Color) On-top view of the center of the (111)-oriented surface of the silver model crystal. The three uppermost atomic layers (solid circles), the two-dimensional Wigner-Seitz cell (solid line), and the 120 impact points within the irreducible zone of the Wigner-Seitz cell (small solid circles) are depicted. In addition, each impact point is colorized according to its individual sputter yield Y.

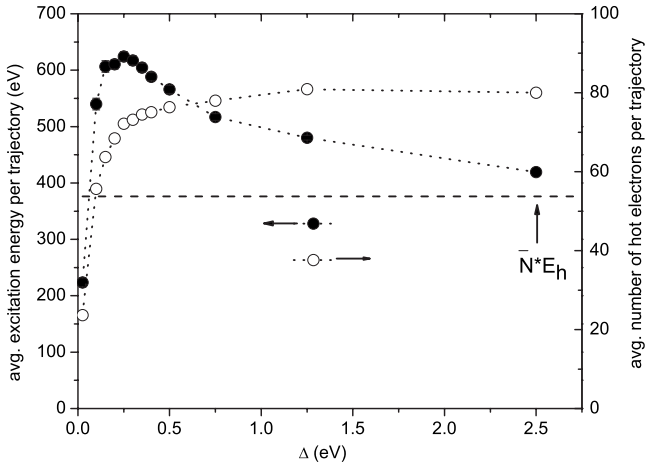

FIG. 3. Average total excitation energy (left) and average number of hot electrons (right) per trajectory for different level widths Δ.

of impact points to an irreducible triangle located within the two-dimensional Wigner-Seitz cell (see Fig. 2). We have chosen a total number of 120 different impact points equidistantly arranged within that irreducible zone.

In addition to the geometry of the impact zone, Fig. 2 shows the obtained sputter yield Y for each impact point (for details on the employed identification scheme for sputtered particles see Ref. 43). The range of calculated yields varies from $Y=0$ up to a maximum observed yield of $Y=29$. The average sputtering yield $\bar{Y}$ is 11.5 and, thus, it is significantly reduced in comparison with previous MD calculations ($\bar{Y} \approx 18$) that neglect electronic energy losses within the atomic-collision cascade. The yield reduction of about 38% that has been found here is slightly larger than the results of Shapiro and Tombrello,[32] who reported yield reductions of about 30% for rather similar model systems. This difference may be due to the fact that Shapiro and Tombrello have only taken into consideration the hole formation during collisional excitation thereby neglecting the hot-electron generation. The latter—as it will be shown later—should be accounted for as an additional sink of kinetic energy that may induce a more pronounced reduction of the average sputtering yield, as found in Ref. 32).

Now, focusing on hot-electron generation by electron promotion, we first have to consider the line width Δ of the promoted diabatic orbital, which determines the transition rate Γ as outlined in the previous section. Unfortunately, theoretical studies of the width Δ seem to be completely lacking for our system. There exist, however, high-resolution photoemission measurements on Pt/Ag(110) that have been performed in experiments by Roy *et al.*[50] By means of photoemission spectroscopy on clean Ag(110), as well as on Pt/Ag(110), level widths of Pt $5d$ resonances have been extracted from the measured density of states for different degrees of Pt coverage Θ. An extrapolation of the experimental data for $\Theta \rightarrow 0$ corresponding to a single absorbed Pt atom on the silver surface yields a resonance width of approximately 0.3 eV. This value we presume as a rough estimate defining the order of magnitude of Δ.

In view of the fact that the exact value of Δ constitutes a parameter that is afflicted with a high degree of uncertainty, the 120 trajectory calculations have been carried out for different resonance widths Δ covering a range from 0.025 to 2.5 eV.

Figure 3 shows the average total excitation energy per trajectory $\bar{E}_t = \Sigma_k E_{\mathrm{exc}}^{(k)}/N$ (k: index of impact point, N: total number of impact points) as a function of the level width Δ.

In the limiting case $\Delta \rightarrow 0$ the energy $\bar{E}_t$ approaches zero, since the lifetime $\tau = 1/\Gamma$ of the electron in the virtual bound state becomes large compared to the typical duration of the atomic collision.

For large resonance widths, however, the lifetime becomes small in comparison with the time window of the close collision, leading to an electronic transition from the VBS into a free conduction-band state directly at the Fermi edge. In that case $\bar{E}_t$ converges toward $\bar{N} \cdot E_h$, with $\bar{N}$ denoting the average number of generated d holes per atomic-collision cascade. With $\bar{N}=80$, this energy is depicted as a dotted line in Fig. 3.

Between these two limiting cases, we observe a maximum of $\bar{E}_t \approx 650$ eV for a level width of 0.25 eV. This value corresponds to about 15% of the total bombarding energy originally imparted into the solid. Furthermore, the data indicate a rather weak dependence of $\bar{E}_t$ on Δ in the proximity of the maximum. Therefore, all calculations to be presented in the following were carried out for a constant-level width of $\Delta = 0.25$ eV.

In order to study the role of the lateral position on the surface the projectile is aimed at, Fig. 4 gives a breakdown of the average total excitation energy $\bar{E}_t$ into the total excitation energies $E_{\mathrm{exc}}^{(k)}$ for each impact point k. Due to the fact that a two-dimensional color representation of data as employed in Fig. 2 would be too indistinct, we have chosen a bar diagram depiction, here. The mapping from the index k

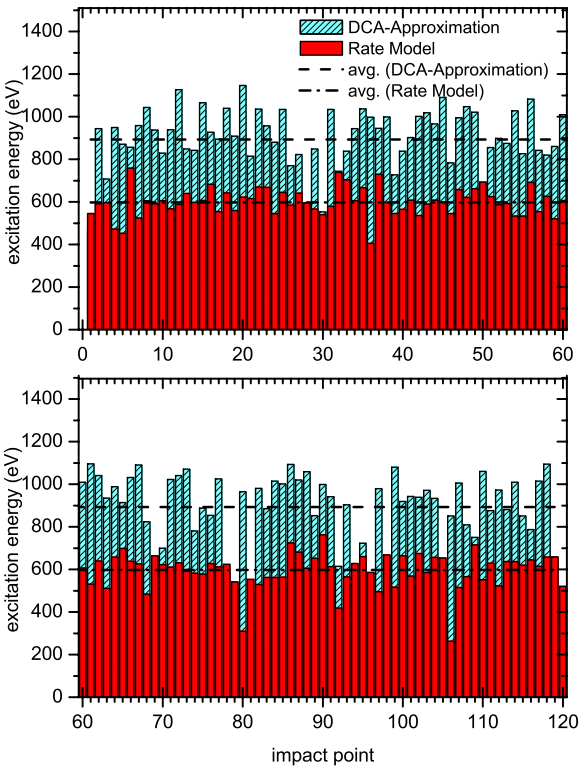

FIG. 4. (Color online) Total excitation energy generated by electron promotion as a function of impact point (additionally see Fig. 5).

to the geometrical position of the corresponding impact point within the irreducible triangle (see Fig. 2) is provided by Fig. 5. For the constant-rate model ($\Delta=0.25$ eV) we observe an average total excitation energy of $\bar{E}_t \approx 600$ eV that is about 2/3 compared to the value of 900 eV obtained within the framework of the DCA approximation. Concerning the individual choice of impact point, the two models yield standard deviations for $\bar{E}_t$ of $\sigma \approx 70$ eV (rate model) and $\sigma \approx 160$ eV (DCA approximation), respectively. Furthermore,

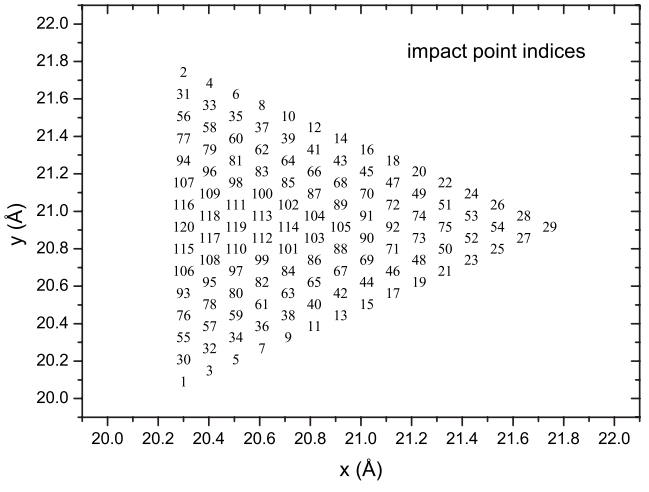

FIG. 5. Mapping from the index k to the location of the corresponding impact point within the irreducible zone of the two-dimensional Wigner-Seitz cell.

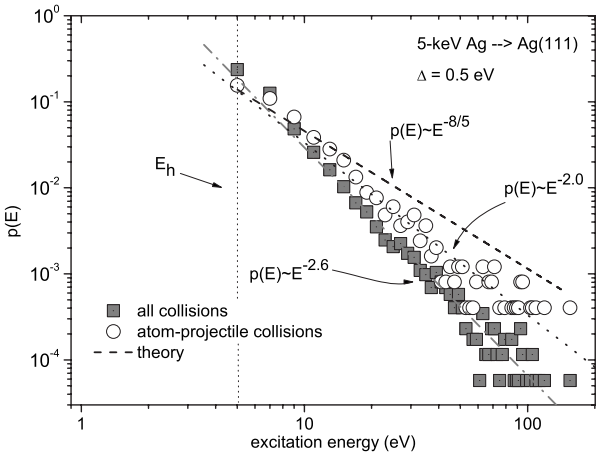

FIG. 6. Nascent excitation energy distribution of hot electrons generated in electron promotion events. The data has been taken from the set of 120 trajectories

by comparing the individual excitation energies from the rate model with those from the DCA model, it becomes obvious that the transition from one model to the other cannot be treated by means of a linear scaling. Thus, the introduction of a constant transition rate does not only alter the amount of energy that is transferred during a hard collision but also significantly influences the evolution of the atomic collision cascade.

Figure 6 shows the excitation energy distribution $f(E_{\mathrm{exc}})$ of hot electrons generated in inelastic collisions comprising (i) all detected hard collisions and (ii) only those collisions the projectile is involved in. Both distributions have been obtained by binning the excitation events into equidistant energy intervals of 2 eV widths. Note, that $f(E_{\mathrm{exc}})$ is normalized such that $\int_0^\infty f(E_{\mathrm{exc}})dE_{\mathrm{exc}}=1$.

We observe that the individual excitation events cover an energy range from E_h up to a maximum of 160 eV. The reader should be aware that hot electrons with an excitation energy exceeding the work function of silver must not generally be assumed to be emitted from the surface since the direction of propagation is undetermined and further scattering processes have to be taken into account. An interesting observation arising from Fig. 6 is that both distributions closely resemble an inverse power law $f(E_{\mathrm{exc}}) \propto E_{\mathrm{exc}}^{-\delta}$ with $\delta \approx 2.6$ (for all collisions) and $\delta \approx 2.0$ (for projectile-atom collisions).

In order to derive an upper estimate for the exponent δ from analytical theory, we may assume that the particle dynamics follow the laws of a *linear-collision cascade*. This basically means that all collisions are assumed to involve one *moving* atom and an atom at rest. In that idealized case the kinetic energy distribution can be approximated by $1/E^2$.[51] By inverting the pair contribution of the many-body MD/MC-CEM potential, the kinetic-energy distribution can be converted into a probability distribution of distances of closest approach and, thus, within the framework of the DCA approximation into an excitation energy distribution of hot electrons (labeled as "theory" in Fig. 6) using Eq. (1). The

distribution resulting from the above procedure is also a power law, however, with a reduced exponent $\delta \approx -8/5$.

IV. CONCLUSION

We have presented a model to incorporate electron promotion into molecular dynamics simulations of atomic-collision cascades in metals. An exemplary application of the model to collision cascades induced by the impact of a 5 keV silver atom onto a Ag(111) surface reveals that about 15% of the total bombarding energy is converted into electronic excitation by electron promotion. Furthermore, a nascent energy spectrum of hot electrons generated during close atomic collisions has been calculated. The spectrum closely resembles a power law $f(E_{\mathrm{exc}}) \propto E_{\mathrm{exc}}^{-\delta}$ with exponents $\delta \approx 2-3$.

ACKNOWLEDGMENTS

The authors would like to thank the Deutsche Forschungsgemeinschaft for financial support within the framework of the Sonderforschungsbereich 616 entitled "Energy Dissipation at Surfaces". We are also indebted to B.J. Garrison for providing the basis of the molecular dynamics code. We also thank Z. Sroubek, M. Schleberger, and D. Diesing for fruitful discussions.

[1] A. Wucher, Mat. Fys. Medd. K. Dan. Vidensk. Selsk. **52**, 405 (2007).
[2] H. Urbassek, Mat. Fys. Medd. K. Dan. Vidensk. Selsk. **52**, 433 (2007).
[3] P. Sigmund, Phys. Rev. **184**, 383 (1969).
[4] A. Duvenbeck, O. Weingart, V. Buss, and A. Wucher, New J. Phys. **9**, 38 (2007).
[5] R. A. Baragiola, Nucl. Instrum. Methods Phys. Res. B **78**, 223 (1993).
[6] S. Meyer, D. Diesing, and A. Wucher, Phys. Rev. Lett. **93**, 137601 (2004).
[7] A. Wucher, Appl. Surf. Sci (to be published 2008).
[8] M. Yu, *Sputtering by Particle Bombardment III* (Springer-Verlag, Berlin, 2001), Chap. 3, pp. 91–154.
[9] A. Benninghoven, F. G. Rudenauer, and H. W. Werner, *Secondary Ion Mass Spectrometry: Basic Concepts, Instrumental Aspects, Applications and Trends* (Wiley, New York, 1987).
[10] J. Schou, Phys. Rev. B **22**, 2141 (1980).
[11] Z. Sroubek, Spectrochim. Acta, Part B **44B**, 317 (1989).
[12] Z. Sroubek, Appl. Phys. Lett. **45**, 849 (1984).
[13] Z. Sroubek, Phys. Rev. B **25**, 6046 (1982).
[14] Z. Sroubek, K. Zdansky, and J. Zavadil, Phys. Rev. Lett. **45**, 580 (1980).
[15] J. K. Norskov and B. I. Lundqvist, Phys. Rev. B **19**, 5661 (1979).
[16] D. Newns, K. Makoshi, R. Brako, and J. van Wunnik, Phys. Scr. **T6**, 5 (1983).
[17] N. D. Lang, Phys. Rev. B **27**, 2019 (1983).
[18] D. V. Klushin, M. Y. Gusev, S. A. Lysenko, and I. F. Urazgildin, Phys. Rev. B **54**, 7062 (1996).
[19] J. Geerlings, J. Los, J. Gauyacq, and N. Temme, Surf. Sci. **172**, 257 (1986).
[20] R. Brako and D. Newns, Vacuum **32**, 39 (1982).
[21] M. Lindenblatt, E. Pehlke, A. Duvenbeck, B. Rethfeld, and A. Wucher, Nucl. Instrum. Methods Phys. Res. B **246**, 333 (2006).
[22] I. Stich, R. Car, M. Parrinello, and S. Baroni, Phys. Rev. B **39**, 4997 (1989).
[23] J. Lindhard and M. Scharff, Phys. Rev. **124**, 128 (1961).
[24] U. Fano and W. Lichten, Phys. Rev. Lett. **14**, 627 (1965).
[25] P. Joyes, Radiat. Eff. **19**, 235 (1973).
[26] D. Bernado, R. Bhatia, and B. Garrison, Comput. Phys. Commun. **80**, 259 (1994).
[27] D. Bernado and B. Garrison, J. Chem. Phys. **97**, 6910 (1992).
[28] D. Duffy and A. Rutherford, J. Phys.: Condens. Matter **19**, 016207 (2007).
[29] A. Duvenbeck, F. Sroubek, Z. Sroubek, and A. Wucher, Nucl. Instrum. Methods Phys. Res. B **225**, 464 (2004).
[30] A. Duvenbeck and A. Wucher, Phys. Rev. B **72**, 165408 (2005).
[31] I. Koponen and M. Hautala, Nucl. Instrum. Methods Phys. Res. B **90**, 396 (1994).
[32] M. Shapiro and T. Tombrello, Nucl. Instrum. Methods Phys. Res. B **90**, 473 (1994).
[33] M. Shapiro and T. Tombrello, Nucl. Instrum. Methods Phys. Res. B **102**, 277 (1995).
[34] M. Shapiro and T. Tombrello, Nucl. Instrum. Methods Phys. Res. B **94**, 186 (1994).
[35] M. Shapiro and J. Fine, Nucl. Instrum. Methods Phys. Res. B **44**, 43 (1989).
[36] M. Shapiro, T. Tombrello, and J. Fine, Nucl. Instrum. Methods Phys. Res. B **74**, 385 (1993).
[37] I. Wojciechowski and B. J. Garrison, Surf. Sci. **527**, 209 (2003).
[38] A. Caro and M. Victoria, Phys. Rev. A **40**, 2287 (1989).
[39] I. Koponen, Phys. Rev. B **47**, 14011 (1993).
[40] M. M. Jakas and D. E. Harrison, Phys. Rev. B **32**, 2752 (1985).
[41] D. Harrison, Jr., B. Garrison, and N. Winograd, Proceedings of the ASMS, St. Louis, MO, 1978, pp. 198–200.
[42] A. Duvenbeck, M. Lindenblatt, and A. Wucher, Nucl. Instrum. Methods Phys. Res. B **228**, 170 (2005).
[43] M. Lindenblatt, R. Heinrich, A. Wucher, and B. J. Garrison, J. Chem. Phys. **115**, 8653 (2001).
[44] A. Wucher and B. Garrison, Surf. Sci. **260**, 257 (1992).
[45] C. Kelchner, D. Halstead, L. Perkins, and N. W. A. DePristo, Surf. Sci. **310**, 425 (1994).
[46] P. Joyes, in *Ion Surface Interaction, Sputtering and Related Phenomena*, edited by R. Behrisch, W. Heiland, W. Poschenrieder, P. Staib, and H. Verbeek (Gordon and Breach, New York, 1973), pp. 139–146.
[47] J. Zhao, Y. Luo, and G. Wang, Eur. Phys. J. D **14**, 309 (2001).
[48] C. Kittel, *Introduction to Solid State Physics* (Wiley, New York, 1971), p. 249.
[49] H. Nakamura and D. G. Truhlar, J. Chem. Phys. **118**, 6816 (2003).
[50] G. Czapek, A. Federspiel, A. Fluckiger, D. Frei, B. Hahn, C. Hug, E. Hugentobler, W. Krebs, U. Moser, D. Muster, E. Ramseyer, H. Scheidiger, P. Schlatter, G. Stucki, R. Abela, D. Renker, and E. Steiner, Phys. Rev. Lett. **70**, 17 (1993).
[51] J. E. Mahan and A. Vantomme, J. Vac. Sci. Technol. A **15**, 1976 (1997).